Perturbation Independent Decay of the Loschmidt Echo in a Many-Body System

C. M. Sánchez, A. K. Chattah, K. X. Wei, L. Buljubasich, P. Cappellaro, and H. M. Pastawski

Phys. Rev. Lett. **124**, 030601 — Published 21 January 2020

DOI: 10.1103/PhysRevLett.124.030601

Emergent perturbation independent decay of the Loschmidt echo in a many-body system

C. M. Sánchez,[1] A. K. Chattah,[1,2] K. X. Wei,[3,4] L.Buljubasich,[1,2] P. Cappellaro,[5,4] and H. M. Pastawski[1,2]

[1] *Facultad de Matemática, Astronomía, Física y Computación - Universidad Nacional de Córdoba, Córdoba, Argentina*
[2] *Instituto de Física Enrique Gaviola (CONICET-UNC), Córdoba, Argentina*
[3] *Department of Physics, Massachusetts Institute of Technology, Cambridge, MA USA.*
[4] *Research Laboratory of Electronics, Massachusetts Institute of Technology, Cambridge, MA 02139, USA*
[5] *Department of Nuclear Science & Engineering, Massachusetts Institute of Technology, Cambridge, MA USA*

When a qubit or spin interacts with others under a many-body Hamiltonian, the information it contains scrambles progressively. Here, nuclear spins of an adamantane crystal are used as a quantum simulator to monitor such dynamics through out-of-time-ordered correlators (OTOCs). Through a Loschmidt Echo (LE) procedure we asses how weak perturbations degrade the information encoded in these increasingly complex states. Both observables involve the implementation of a time-reversal procedure which, in practice, involves inverting the sign of the effective Hamiltonian. Our protocols use periodic radio frequency pulses that profit from the natural dipolar interaction to implement a Hamiltonian that can be scaled down at will. Meanwhile, experimental errors and strength of perturbative terms remain constant and can be quantified through the LE. In each case, information spreading occurs with a time scale, T_2, inversely proportional to the local second moment of the Hamiltonian. We find that when the reversible interactions dominate over the perturbations, the information scrambled among up to 10^2 spins can still be recovered. However, we find that the LE decay rate can not become smaller than a critical value $1/T_3 \approx (0.15 \pm 0.02)/T_2$, that only depends on the interactions themselves, and not on the perturbations. This result shows the emergence of a regime of intrinsic irreversibility in accordance to a Central Hypothesis of Irreversibility, hinted from previous experiments .

The recent achievements in the preservation and manipulation of complex quantum states bring us ever closer to practical quantum information processing [1]. However, as the number of qubits increases [2–4], it becomes crucial to assess the robustness of multi-qubit superpositions. This also holds for the foundations of quantum statistical mechanics [5–7], the black hole information paradox and the related quantum information roots of space-time geometry [8, 9]. These issues launched a renewed interest on many-body quantum chaos. In particular, the neighborhood of a black hole is maximally chaotic. Thus, a field theory that satisfies the classical/quantum (AdS/CFT) correspondence should be affected by a "quantum butterfly effect" [10–12]. Indeed, for one-body chaotic systems, a semi-classical analysis predicts that the fraction of a quantum excitation recovered under a perturbed time reversal, i.e. a Loschmidt Echo (LE) [13, 14], *decays* with a classical Lyapunov exponent. Such exponent also controls the *growth* of quantum uncertainties evaluated through out-of-time-order correlators (OTOCs) [15, 16]. While some spin Hamiltonians show spectral signatures of chaos [17, 18], they do not have a classical equivalent. Thus, it is not clear whether the expected Lyapunov-like dynamical instability actually holds [10–12]. Besides, one might suspect that such instability could also amplify small errors that could limit the unscrambling process. Indeed, different experiments seem to find an unbeatable limit to the reversibility in spite of their effort to reduce experimental imperfections [19–22]. This led us to formulate a *Central Hypothesis of Irreversibility* [23, 24] stating that, for unbounded systems, there is an intrinsic irreversibility time scale proportional to the scrambling time. Our present work gives definitive support to this statement.

Within solid-state Nuclear Magnetic Resonance (NMR) [25], we engineered periodic sequences of radio frequency (rf) pulses to implement different target dipolar XXZ Hamiltonians and invert their sign allowing time-reversal[26]. This quantum simulator (QS) enables to monitor how information scrambles through an unbounded 3D lattice of interacting spins/qubits under unitary evolution, and how precisely it can be recovered. Indeed, the traditional Magic Echo (ME) [19, 27] and Multiple Quantum Coherence (MQC) experiments [28, 29] inspired the new procedures for LEs and OTOCs[30]. We suspected that our NMR-QS might reveal an emergent behavior of many-body systems, in this case towards intrinsic irreversibility [24] , as it did for Quantum Dynamical Phase Transitions (QDPTs) [21, 31] and other Quantum Phase Transitions (QPT) [32–35].

Thus, by changing the Hamiltonian strength by a scaling factor $\pm\delta$, while keeping the experimental errors nearly constant, we were able to: (i) transform an initially localized spin excitation into a complex multi-spin superposition under the Hamiltonian unitary dynamics while varying its time-scale with respect to that of perturbations and errors, (ii) measure the information scrambling on the unbounded lattice through OTOCs, and (iii) use the LE to quantify the information recovered from these scrambled states under different conditions. We find that information scrambles among a spin cloud that grows diffusively while the LE becomes exponen-

tially small. An intrinsic irreversibility rate, interpreted as the Lyapunov exponent of the spin system, is seen to emerge when the Hamiltonian dominates over the experimental imperfections (Fig.5).

Controlling the many-body dynamics – The $N \approx 10^{23}$ *equivalent* ^{1}H nuclear spins-$\frac{1}{2}$ of polycrystalline adamantane [36], precess at frequency ω_0 under the magnetic field along z of the laboratory xyz-frame. It ensures a thermal state $\rho(0) \approx \mathbb{1} - \beta\omega_0 \sum_i I_i^z$ with $\hbar = 1$, $\beta\omega_0 \approx 10^{-5}$, $1/\beta$ the room temperature and I_i^z, the z component of i-th spin operator. A first $[\frac{\pi}{2}]_x$ rf pulse, dubbed X, creates an excitation by tilting each spin to xy-plane, $I_i^z \to -I_i^y$, where they evolve under the secular dipolar Hamiltonian[37] ,

$$\begin{aligned}\mathcal{H}_{\rm d}^{zz} &= \sum_{i<j} d_{ij}(-I_i^x I_j^x - I_i^y I_j^y + 2I_i^z I_j^z) \\ &= \sum_{i<j} d_{ij}(-\tfrac{1}{2}[I_i^+ I_j^- + I_i^- I_j^+] + 2I_i^z I_j^z),\end{aligned} \tag{1}$$

dubbed XXZ. Here, d_{ij} is a dipolar coupling. Terms of the form $d_{ij}[I_i^+ I_j^+ + I_i^- I_j^-]$ were already truncated as $d_{ij} \ll \omega_0$. Since I_i^y and $\mathcal{H}_{\rm d}^{zz}$ do not commute, the polarization $I^y(t)$ decays in a time $T_2 = 1/\sqrt{M_2}$, with $M_2 = {\rm Tr}[\mathcal{H}^{zz}, I^y]^2/{\rm Tr}[I^y I^y]$ the second moment of the Hamiltonian[38]. After a time τ a new pulse attempts to recover the z polarization yielding $e^{i\frac{\pi}{2}I^x} e^{-i\mathcal{H}_{\rm d}^{zz}\tau} e^{-i\frac{\pi}{2}I^x} I^z = e^{-i\mathcal{H}_{\rm d}^{yy}\tau} I^z$. Thus, the dynamics of each $I_i^y = \frac{1}{2}(I_i^+ - I_i^-)$ under XXZ is fully equivalent to that of I_i^z under XYX, the non-secular Hamiltonian in the *toggling frame*[37],

$$\mathcal{H}_{\rm d}^{yy} = -\tfrac{1}{2}\mathcal{H}_{\rm d}^{zz} - \tfrac{3}{4}\sum_{i<j} d_{ij}[I_i^+ I_j^+ + I_i^- I_j^-]). \tag{2}$$

A sequence of different $\frac{\pi}{2}$ rf pulses and free evolution periods yields, in the Trotter approximation, $e^{[-i\mathcal{H}_{\rm d}^{xx}\tau(1-\delta))]} \times e^{[-i\mathcal{H}_{\rm d}^{zz}\tau])} \times e^{[-i\mathcal{H}_{\rm d}^{yy}\tau(1-\delta))]} \approx e^{[-i\mathcal{H}_{\rm d}^{yy}\tau\delta)]}$. A repetition of this cycle yields an average Floquet Hamiltonian $\mathcal{H}_\delta \simeq \delta\mathcal{H}_{\rm d}^{yy}$ whose strength scales with δ. More precisely, I_i^z evolves under the average Hamiltonian $\mathcal{H}_\delta + \Sigma$, where $\mathcal{H}_\delta$ is, at zeroth order, our engineered Hamiltonian and $\Sigma = \sum_{i=1}^{\infty} \mathcal{H}_\delta^{(i)}$ is a constant perturbation described by the Magnus expansion, whose strength does not change much with δ [39–41]. For compactness, we include in Σ any other small experimental imperfection. Thus, we designed two sets of periodic trains of $\frac{\pi}{2}$ rf pulses to achieve $-\frac{1}{2} \le \delta \le 1$ while keeping fixed the pulse number and cycle period t_c and thus the experimental errors. The 8-pulse sequences, dubbed **8P$_\delta$-F**, for **F**orward, and **8P$_\delta$-B**, for **B**ackward, are shown in Fig. 1. The other two, **16P$_\delta$-F** and **16P$_\delta$-B**, repeat the cycle t_c with opposite phases, cancelling all odd-order corrections in Σ. Both cancel out the Zeeman terms. We simplify the notation by saving obvious indices and making explicit

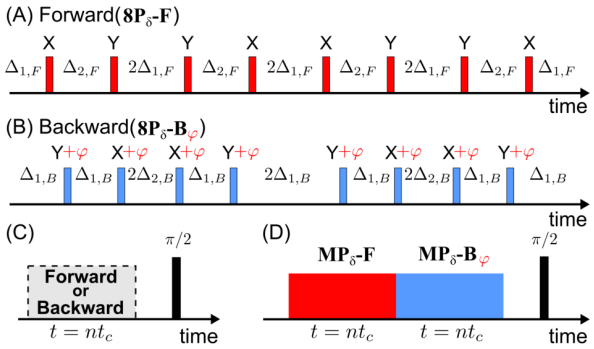

FIG. 1. **Scaled XYX dynamics $\delta\mathcal{H}_d^{yy}$.** (A) Forward and (B) backward 8-pulse sequences, (**8P$_\delta$-F** and **8P$_\delta$-B**), consist of $\frac{\pi}{2}$ rf pulses along X or Y. The inter-pulse delays $\Delta_{1,F} = \tau(1-\delta)$, $\Delta_{2,F} = \tau(1+2\delta)$, $\Delta_{1,B} = \tau(1+\delta)$, $\Delta_{2,B} = \tau(1-2\delta)$, a cycle is $t_c = 12\tau$. An evolution time t, requires $n = t/t_c$ cycles. In **8P$_\delta$-B**, pulses are rotated by φ . (C) **Polarization Dynamics** $\langle I^z(t) I^z(0)\rangle_\beta$. The longitudinal total magnetization is probed after a last $\pi/2$ pulse. [41]. (D) **Loschmidt echo (LE),** $M^\delta(t)$, concatenates the forward, **8P$_\delta$-F**, and backward, **8P$_\delta$-B**, dynamics. **OTOC protocol**. It inserts a perturbation, $\Phi = e^{iI^z(t)\varphi}$, before time reversal, achieved by shifting all pulses in the backward block by φ to get. $S_\varphi(t) = \langle\Phi^\dagger(t) I_0^z(0)\Phi(t) I_0^z(0)\rangle_\beta$ with $S_{\varphi=0}(t) \equiv M^\delta(t)$.

the sign of the scaling of the acting XYX Hamiltonian: $\mathcal{H}_{\delta,F(B)} = \pm\mathcal{H}_\delta + \Sigma = \pm\delta\,\mathcal{H} + \Sigma$. Our experiments start with the non-equilibrium polarization I^z along the *new* z-axis where it evolves under $\pm\delta\mathcal{H}$, the scaled XYX (see Fig. 1 C). As the sequence ends at time t, the polarization $I^z(t)$ rests along the *laboratory* z (see [41]) and it is recorded as a standard time-ordered correlation function:

$$\begin{aligned}P^\delta(t) &= \langle e^{i\mathcal{H}_{\delta,F(B)}t} I^z e^{-i\mathcal{H}_{\delta,F(B)}t} I^z\rangle_\beta = \langle I^z(t) I^z(0)\rangle_\beta \\ &= \sum_{j,i} \langle I_j^z(t) I_i^z(0)\rangle_\beta.\end{aligned} \tag{3}$$

Here, $\langle\cdot\rangle_\beta$ denotes the expectation on the thermal state, normalized to its value at $t = 0$. $P^\delta(t)$ decays with a rate $1/T_2$ which already hints at, but does not quantifies, its scrambling. A first Trotter time step , $I_i^z(\tau) \approx I_i^z(0)\cos[\tau/T_2] - i[\mathcal{H}_\delta, I_i^z(0)]\sin[\tau/T_2]$, at $\tau = \frac{\pi}{2}T_2$ shows that after n steps $I^z(t)$ scrambles as *coherences*, i.e. a superposition of different K-spin operators, say $I_l^- I_k^+ I_i^z \cdots$, each of them decaying in a time of about $T_2/\sqrt{K}$. [29, 42]. A small n suffices for the phases to become pseudo-random and suppress quantum interferences. Thus, the decay pathways in the Liouville space can be viewed as a set of discrete-time random walks or particles falling in a Galton's board, justifying its interpretation as "equilibration"[7, 43].

Scaled dynamics – Our protocols were tested by measuring $P^\delta(t)$ which slow down as δ decreases (Fig. 2) and, most crucial for LE and OTOCs, they show identical

forward and backward dynamics. Ideally, $P^{\delta=0}(t)$ should not evolve[25]. Instead, its decay reveals the effect of Σ . The 16-pulse sequence exactly *cancels out all odd-order* terms in Σ, giving longer coherence times at $\delta = 0$, while the evolution for $\delta > 0$ yields similar results to $\mathbf{8P}_\delta$ [41]. This shows that $\mathcal{H}^{(0)}$ is a good approximation to the acting Hamiltonian in both cases. We use $\mathbf{8P}_\delta$**-F,B** to monitor fast dynamics as it allows more frequent observations.

The reliability of the scaling is quantified in Fig. 2 by P^δ as a function of the *self-time*, $\delta t = \delta \times t$. Remarkably, all data collapse into a single curve with a characteristic oscillation [38] at around $\delta t \approx 100$ μs that describes a non-secular dipolar dynamics [38], $P(t) = \mathrm{sinc}[wt]\exp[-(ht)^2/2]$. This yields the Hamiltonian second moment $M_2 = (1/T_2)^2$ and its corresponding relaxation time , $1/T_2 = \sqrt{h^2 + w^2/3}$, linear in δ (as shown in [41]). This trend continues for $\delta = 0.1$ and below. $P^\delta(\delta t)$ also coincides with a *free evolution* of I^z under $\mathcal{H}_\mathrm{d}^{yy}$ (i.e. $\delta = 1$), and under a continuous *high power irradiation* as in the ME [19], ($\delta = -\frac{1}{2}$). For the smaller δ the oscillations smear out because of the longer experimental time required for the same self-time.

Time reversal, OTOCs and spin counting – The combination of a forward and backward dynamics (Fig. 1.D) for the same self-time $\delta \times t$, yields the LE:

$$M^\delta(t) = \sum_{j,i} \langle e^{+\mathrm{i}t\mathcal{H}_{\delta,F}} e^{+\mathrm{i}t\mathcal{H}_{\delta,B}} I_j^z e^{-\mathrm{i}t\mathcal{H}_{\delta,B}} e^{-\mathrm{i}t\mathcal{H}_{\delta,F}} I_i^z \rangle_\beta \approx \langle e^{+\mathrm{i}t\mathcal{H}_{\delta,F}} e^{+\mathrm{i}t\mathcal{H}_{\delta,B}} I_0^z e^{-\mathrm{i}t\mathcal{H}_{\delta,B}} e^{-\mathrm{i}t\mathcal{H}_{\delta,F}} I_0^z \rangle_\beta \quad (4)$$

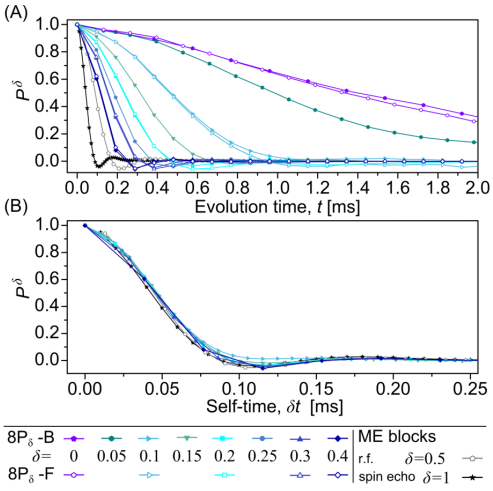

FIG. 2. **Polarization dynamics**: (A) Forward and backward evolution, (B) backward evolution as a functions of *self-time*, $\delta t = \delta \times t$. Scaled dynamics are obtained with the $\mathbf{8P}_\delta$ sequences for $|\delta| \in [0, 0.4]$ and the ME forward, $\delta = 1$ (spin-echo) and backward $\delta = 0.5$ (on-resonance irradiation) portions.

Only if $\Sigma = 0$ to all orders does the LE become perfect, $M^\delta(t) \equiv 1$. Thus, the irreversibility is quantified by the *LE decay time* T_3^δ, defined as by $M^\delta(T_3^\delta) = 1/2$. The scrambling of $I^z(t)$ can be monitored by an instantaneous spin rotation $\Phi = e^{-i\varphi I^z}$ that labels portions of the Hilbert space according to their spin projection. Let's assume that $\Sigma = 0$ in Eq. 4 except at the beginning of time reversal, when Φ perturbs $I^z(t)$. Thus, the LE depends on φ. Identifying $\Phi(t) = e^{\mathrm{i}t\mathcal{H}} e^{-i\varphi I^z} e^{-\mathrm{i}t\mathcal{H}}$ we write the LE as an OTOC:

$$S_\varphi(t) = \sum_{j,i} \langle \Phi^\dagger(t) I_j^z \Phi(t) I_i^z \rangle_\beta \approx \langle \Phi^\dagger(t) I_0^z(0) \Phi(t) I_0^z(0) \rangle_\beta . \quad (5)$$

By repeating for $\varphi_n = 2\pi n/Q$, $n = 0, 1, ..., Q-1$, we get[27] $S_q^\delta(t) = \sum_{n=0}^{Q-1} e^{\mathrm{i}q\varphi_n} S_{\varphi_n}^\delta(t)$. Each S_q sums up of all the strengths $|\langle m_z'|I^z(t)|m_z\rangle|^2$ describing superpositions with spin projections m_z and m_z' with $|m_z - m_z'| = q$, i.e. the *coherences* of order q [44] While the sum of MQC intensities yields the LE, their second moment, $\mathcal{Q}^2 = \sum_q q^2 S_q(t)$ is the expectation value of a squared commutator [30, 45, 46], $\mathcal{C}_{zz}(t) = \langle |[I^z(t), I^z(0)]|^2 \rangle_\beta \propto \mathcal{Q}^2$. The pseudo-random phases smooths the oscillations of MQC intensities, enabling a combinatorial analysis that associates their distribution at a given time, t, with the number K of spin operators with a coherence q as $(2K)!/[(K+q)!(K-q)!]$ approximated by $S_q(K) \propto e^{-q^2/K}$. *Spin counting* [44] is to fit its width as the number of spins effectively entangled $N(t) = \mathcal{Q}$ [42].

By implementing **16P-F** and **16P-B**, we extracted the normalized OTOC intensities $S_q^\delta(t)$ for several scaling factors and evolution times. Fig. 3 shows the number of correlated spins N as a function of the self-time. All the data fall into a single curve $N(\delta t) \sim (\delta t)^{3/2}$. This indicates that each $I_i^z(0)$ scrambles into multi-spin states within a spin cloud whose radius grows diffusively. This unbounded growth differs from and the linear growth recently observed in linear chains [35]. It also contrasts with the exponential growth of $N(t)$ seen in adamantane[34, 42] under the "ballistic" dynamics of

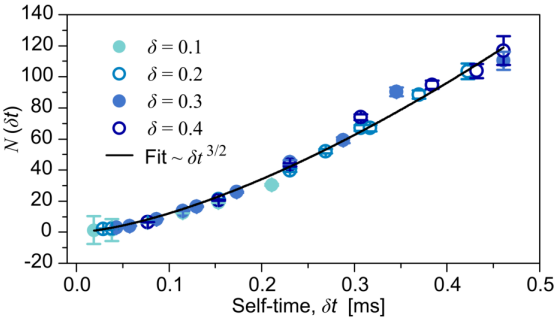

FIG. 3. **Scrambling growth** from OTOCs using the 16-pulse sequence for different δ . The number of correlated spin $N(\delta t)$ (circles) fit a power law (black solid line), $N(\delta t) = A\,\delta t^b$, with $b = 1.49 \pm 0.04$.

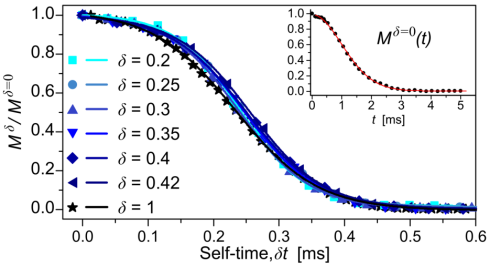

FIG. 4. **Loschmidt Echo decay** normalized by $M^{\delta=0}(t)$ in the inset, as a function of self-time, using the $\mathbf{8P}_\delta$ sequence, for different δ. Lines are fits to a sigmoid.

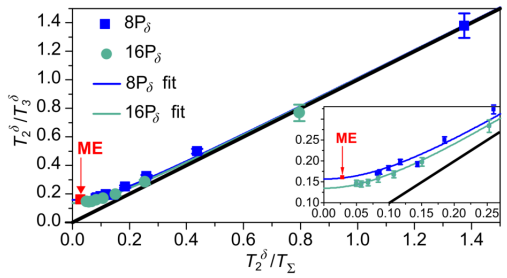

FIG. 5. Scaled LE decay rates T_2^δ/T_3^δ vs. perturbation rate T_2^δ/T_Σ, for $\mathbf{8P}_\delta$ (blue) and $\mathbf{16P}_\delta$ (green). Also shown is the ME result ($\delta = 0.5$, red). Blue and green lines are fits to the function $(T_2^\delta/T_3^\delta) = \sqrt{R^2 + (T_2^\delta/T_\Sigma)^2}$.The black line is a guide to the eye. The inset is a zoom in the region of saturation of (T_2^δ/T_3^δ).

$\mathcal{H}_{2Q} \propto \sum_{i<j} d_{ij}[I_i^+ I_j^+ + I_i^- I_j^-]$). This confirms the disruptive role of the many-body effects of $I_i^z I_j^z$, which lead to MBL when they dominate [5, 7, 35, 47]. The usual discussions of MQC and OTOCs assume [30, 44] a perfect time reversal $\mathcal{H}_{\delta,F} = -\mathcal{H}_{\delta,B}$, but they work even under $\Sigma \neq 0$. We may understand why by noting that the initial state is a set of *independent* (i.e. incoherent) of equivalent spin excitations I_i^z, the *pseudo-pure states*.[48]. Since each of them scrambles into a coherent superposition in a time scale T_2 [27, 42, 44], we may focus on one of them, say $I_0^z(t)$. The time reversal after the Φ perturbation cannot fully undo its dynamics. Thus, a substantial number of backward paths in the Liouville space do not lead to I_0^z but remains as multi-spin superposition without net z-polarization [12, 29]. Thus, the observed polarization after a LE, corresponds to the small portions of paths that has unscrambled the multi-spin correlation into its original $I_0^z(0)$ [29]. While the intensity $S_\varphi(t)$ is further diminished by the imperfection Σ this is compensated by a normalization with the LE $S_{\varphi=0}(t)$ which does not affect its dependence on φ.[27, 42]. Thus, one can safely remove the sum over j in Eq.5 justifying the approximations in Eqs.4 and 5. This means that the *normalized* OTOC, $S_\varphi(t)$, describes the probability that a *local* excitation at the 0-th spin returns to its origin , when *only* Φ prevents a perfect time reversal.

Loschmidt echoes – We may finally focus on the crucial question of how a constant Σ limits the recovery of quantum information scrambled into a multi-spin system. Σ can be quantified using $M^{\delta=0}(t)$. Its decay (see inset of Fig. 4), fits a model [24, 49, 50] that interpolates between an initial Gaussian (dubbed quantum Zeno regime) and a Fermi Golden Rule decay $M^{\delta=0}(t) = \exp\left[2\frac{\Gamma^2}{\sigma^2} - 2\sqrt{\frac{\Gamma^4}{\sigma^4} + \Gamma^2 t^2}\right]$ (red line in inset of Fig. 4; details in [41]). Its half maximum intensity defines the time scale associated with the time reversal imperfection, $T_\Sigma = T_3^{\delta=0}$. For $\delta > 0$, we observe that LE data, normalized by $M^{\delta=0}(t)$, overlap when plotted as function of the *self-time* (Fig. 4). The decay can be best fitted to a sigmoid, $(1 + e^{\lambda(t-t_s)})^{-1}$, underlying an initial slow decay before the exponential dominates [41]. This law was first found for a ME experiment [51] and only then identified in the LE in a 2D gas of rigid spheres[52], where $1/t_s$ depends on the perturbation strength and λ is a *Lyapunov* exponent. Thus, our experimental rate $1/T_3^\delta$ accounts for both time scales. Strikingly, the tendency of $M^\delta(\delta t)/M^{\delta=0}(\delta t)$ to overlap for the bigger δ unveils that all the irreversibility rates $1/T_3^\delta$, as well as λ, tend to be proportional to δ, i.e. to the Hamiltonian. This suggests [24] a plot of the normalized decay rate, T_2^δ/T_3^δ, versus the perturbation's characteristic rate T_2^δ/T_Σ. All pulse sequences used here ($\mathbf{8P}_\delta$, $\mathbf{16P}_\delta$, and ME) fall in a universal curve (Fig. 5) despite of the different origin of their Σ. At small δ, Σ dominates over the intrinsic dipolar dynamics, $T_2^\delta/T_\Sigma \gg 1$ and hence the experimental points fall on a line with unit slope ($T_3^\delta \approx T_\Sigma$). For larger δ, the reversible interactions become dominant, $T_2^\delta/T_\Sigma \ll 1$. Strikingly, the ratio T_2^δ/T_3^δ does not vanishes but saturates at the critical fraction $R \approx 0.15 \pm 0.02$. This holds for Σ's with different strengths and nature: **8P** , **16P**, ME and a mixture of them. In this weak perturbation limit, the *"reversible" interactions* producing the scrambling, *also determine an intrinsic irreversibility rate.*

Conclusions – By scaling down a XXZ Hamiltonian and inverting its sign, we measured, through OTOCs, the information scrambling and, through the LE, how much of this information is recoverable. Indeed scrambling dynamics depends on the system, the initial state, the observable and the specific Hamiltonian. For our system, $I_0^y(t)$ under dipolar XXZ dynamics [17, 18], does not scramble exponentially, as might be expected[10], but with a diffusive power law. Nevertheless, the "butterfly effect", manifests in the exponential decay of the LE. However, being this decay rate $\lambda \propto T_2 \ll 1/\beta$, it confirms that XXZ falls short[11] from the strong chaos required for a quantum many-body system to satisfy the AdS/CFT correspondence[10, 11].

By reaching the regime where the spin-spin dynamics dominates over the perturbations we found an intrinsic upper bound for LE decay time $T_3^\delta \leq T_2^\delta/R$. This,

demonstrates the validity of our *Central Hypothesis of Irreversibility* stating that for weak perturbations *the LE decays with a perturbation-independent ratethat is proportional to the local second moment of the unperturbed Hamiltonian*. Thus, $1/T_3$ plays the role of the Lyapunov exponent in semi-classical limit, where weak perturbations control a FGR decay of the LE but a Lyapunov decay manifests for $\Sigma \geq \Sigma_c$ [13, 14]. The present observation of $\Sigma_c = 0$ becomes conceivable[53, 54] in the thermodynamic limit of $N \to \infty$ and then $\Sigma \to 0$. Thus, it seems that we are in presence of a Quantum Dynamical Phase Transition [21, 24, 31] where the perturbation dependent range [14] collapses yielding intrinsic irreversibility. This could be seen as a departure from unitary quantum dynamics with strong implications for the black hole information paradox [10].

Finally, the perturbation-independent time scale of the LE decay seems to set a limit to the retrieval of information scrambled as complex superpositions and to its preservation from thermalization. However, the decay is neither an exponential [13] nor a Gaussian [21, 55], but a sigmoid [51]. This indicates that in many-body systems far from equilibrium information remains fairly retrievable at the initial stages. This should allow the implementation of error correcting protocols, as it is only after a few times T_2 that the scrambling becomes irreversible to all practical purposes.

Dedicated to the memory of Patricia Rebeca Levstein.

[1] C. R. Monroe, R. J. Schoelkopf, and M. D. Lukin, Sci. Amer. **314**, 50 (2016).
[2] J. Zhang, P. W. Pagano, G. Hess, A. Kyprianidis, P. Becker, H. Kaplan, A. V. Gorshkov, and C. Gong, Z.-X. and-Monroe, Nature **551**, 601 (2017).
[3] H. Bernien, S. Schwartz, A. Keesling, H. Levine, A. Omran, H. Pichler, S. Choi, A. S. Zibrov, M. Endres, M. Greiner, V. Vuletić, and M. D. Lukin, Nature **551**, 579 (2017).
[4] C. Neill, P. Roushan, K. Kechedzhi, S. Boixo, S. V. Isakov, V. Smelyanskiy, A. Megrant, B. Chiaro, A. Dunsworth, K. Arya, R. Barends, B. Burkett, Y. Chen, Z. Chen, A. Fowler, B. Foxen, M. Giustina, R. Graff, E. Jeffrey, T. Huang, J. Kelly, P. Klimov, E. Lucero, J. Mutus, M. Neeley, C. Quintana, D. Sank, A. Vainsencher, J. Wenner, T. C. White, H. Neven, and J. M. Martinis, Science **360**, 195 (2018).
[5] D. M. Basko, I. L. Aleiner, and B. L. Altshuler, Ann. Phys. **321**, 1126 (2006).
[6] J.-Y. Choi, S. Hild, J. Zeiher, P. Schauß, A. Rubio-Abadal, T. Yefsah, V. Khemani, D. A. Huse, I. Bloch, and C. Gross, Science **352**, 1547 (2016).
[7] F. Borgonovi, F. M. Izrailev, L. F. Santos, and V. G. Zelevinsky, Phys. Rep. **626**, 1 (2016).
[8] F. M. Pastawski, B. Yoshida, D. Harlow, and J. Preskill, J. High Energ. Phys. **149**, 2015 (2015).
[9] R. Cowen, Nature **527**, 290 (2015).
[10] J. Maldacena, S. H. Shenker, and D. Stanford, J. High Energ. Phys. **2016**, 106 (2016).
[11] A. Kitaev, in *Brown Phys. Colloq., March 6* (2017).
[12] B. Swingle, Nat. Phys. **14**, 988 (2018).
[13] R. A. Jalabert and H. M. Pastawski, Phys. Rev. Lett. **86**, 2490 (2001).
[14] F. M. Cucchietti, H. M. Pastawski, and R. A. Jalabert, Phys. Rev. B **70**, 035311 (2004), (see Figs. 4, 5 and 6).
[15] A. I. Larkin and Y. N. Ovchinikov, Sov.Phys. JETP **28**, 1200 (1969).
[16] E. B. Rozenbaum, S. Ganeshan, and V. Galitski, Phys. Rev. Lett. **118**, 086801 (2017).
[17] P. van Ede van der Pals and P. Gaspard, Phys. Rev. E **49**, 79 (1994).
[18] D. Jyoti, ArXiv:1711.01948 (2017).
[19] W.-K. Rhim, A. Pines, and J. S. Waugh, Phys. Rev. B **3**, 684 (1971).
[20] S. Zhang, B. H. Meier, and R. R. Ernst, Phys.Rev.Lett. **69**, 2149 (1992).
[21] P. R. Levstein, G. Usaj, and H. M. Pastawski, J. Chem. Phys. **108**, 2718 (1998).
[22] H. M. Pastawski, P. R. Levstein, G. Usaj, J. Raya, and J. Hirschinger, Physica A **283**, 166 (2000).
[23] P. R. Zangara, D. Bendersky, P. R. Levstein, and H. M. Pastawski, Phil. Trans. Royal Soc. A **374**, 20150163 (2016).
[24] P. R. Zangara and H. M. Pastawski, Phys. Scr. **92**, 033001 (2017).
[25] J. S. Waugh, L. M. Huber, and U. Haeberlen, Phys. Rev. Lett. **20**, 180 (1968).
[26] E. Hahn, Phys. Rev. **80**, 580 (1950).
[27] C. M. Sánchez, P. R. Levstein, L. Buljubasich, H. M. Pastawski, and A. K. Chattah, Phil. Trans. Royal Soc. A **374**, 20150155 (2016).
[28] M. Munowitz and A. Pines, Science **233**, 525 (1986).
[29] H. Cho, T. Ladd, J. Baugh, D. Cory, and C. Ramanathan, Phys. Rev. B **72**, 054427 (2005).
[30] J. Cohn, A. Safavi-Naini, R. J. Lewis-Swan, J. G. Bohnet, M. Gärttner, K. A. Gilmore, J. E. Jordan, A. M. Rey, J. J. Bollinger, and J. K. Freericks, New J. Phys. **20**, 055013 (2018).
[31] G. A. Álvarez, E. P. Danieli, P. R. Levstein, and H. M. Pastawski, J. Chem. Phys. **124**, 194507 (2006).
[32] P. Zanardi, H. T. Quan, X. Wang, and C. P. Sun, Phys. Rev. A , 032109 (2007).
[33] J. Zhang, X. Peng, N. Rajendran, and D. Suter, Phys. Rev. Lett. **100**, 100501 (2008).
[34] G. A. Álvarez, D. Suter, and R. Kaiser, Science **349**, 846 (2015).
[35] K. X. Wei, C. Ramanathan, and P. Cappellaro, Phys. Rev. Lett. **120**, 070501 (2018).
[36] I. Schnell and H. W. Spiess, J. Magn. Reson. **151**, 153 (2001).
[37] C. P. Slichter, *Principles of magnetic resonance* (Springer-Verlag, Berlin; New York, 1990).
[38] A. Abragam, *Principles of Nuclear Magnetism*, reprinted ed. (Oxford Univ. Press, 2007).
[39] U. Haeberlen, *High Resolution NMR in solids* (Academic Press, 1976).
[40] R. R. Ernst, G. Bodenhausen, and A. Wokaun, *Principles of nuclear magnetic resonance in one and two dimensions* (Oxford Univ. Press, Oxford, 1987).
[41] Supplementary Material at [URL will be inserted by pub-

lisher] for details on methods and experiments.
[42] C. M. Sánchez, R. H. Acosta, P. R. Levstein, H. M. Pastawski, and A. K. Chattah, Phys. Rev. A **90**, 042122 (2014).
[43] P. R. Zangara, A. D. Dente, E. J. Torres-Herrera, H. M. Pastawski, A. Iucci, and L. F. Santos, Phys. Rev. E **88**, 032913 (2013).
[44] M. Munowitz, A. Pines, and M. Mehring, J. Chem. Phys. **86**, 3172 (1987).
[45] A. K. Khitrin, Chem. Phys. Lett. **274**, 217 (1997).
[46] K. X. Wei, P. Peng, O. Shtanko, I. Marvian, S. Lloyd, C. Ramanathan, and P. Cappellaro, Phys. Rev. Lett. **123**, 090605 (2019).
[47] P. R. Zangara, A. D. Dente, A. Iucci, P. R. Levstein, and H. M. Pastawski, Phys. Rev. B **88**, 195106 (2013).
[48] D. G. Cory, A. F. Fahmy, and T. F. Havel, PNAS **94**, 1634 (1997).
[49] V. V. Flambaum and F. Izrailev, Phys. Rev. E **64**, 026124 (2001).
[50] E. Rufeil-Fiori and H. M. Pastawski, Chem. Phys. Lett. **420**, 35 (2006).
[51] E. Rufeil-Fiori, C. M. Sánchez, F. Oliva, H. M. Pastawski, and P. R. Levstein, Phys. Rev. A **79**, 032324 (2009).
[52] R. Pinto, E. Medina, and H. M. Pastawski, BAPS March Meeting , J22.001 (2004).
[53] P. W. Anderson, Science **177**, 393 (1972).
[54] P. R. Zangara, D. Bendersky, and H. M. Pastawski, Phys. Rev. A **91**, 042112 (2015).
[55] W. H. Zurek, F. M. Cucchietti, and J. P. Paz, Acta Phys. Pol. B **38**, 1685 (2007).